A Convection/Radiation Temperature Control System for High Power Density Electronic Device Testing

Matthew Sweetland
e-mail: sweetlan@alum.mit.edu

John H. Lienhard V
e-mail: lienhard@mit.edu

Alexander H. Slocum
e-mail: slocum@mit.edu

Department of Mechanical Engineering,
Massachusetts Institute of Technology,
77 Massachusetts Avenue,
Cambridge, MA 02139-4307

Active control of die-level temperature is required during production testing of high power microprocessors in order to ensure accurate performance classification, but control is becoming more difficult as the device power densities increase. With power densities approaching 100 W/cm^2, the current passive control systems are no longer able to maintain the required temperature tolerance for production testing. This paper describes the design and testing of a temperature control system that combines high performance impingement cooling with higher power laser heating with application to packaged integrated circuit devices under dynamic testing conditions. Also presented are system design concepts and experimental results for typical microprocessor thermal test vehicles. [DOI: 10.1115/1.2966437]

Keywords: temperature control, device under test, convective cooling, radiation heating, laser heating

1 Introduction

The control of die temperature is very important for the accurate classification and testing of high speed microprocessor devices. During the testing process, device manufacturers specify a minimum device temperature with an allowed range of deviation (e.g., 85°C+4°C/−0°C).[1] The higher the temperature deviation above this specified test temperature, the higher the risk of classifying a device in the wrong category due to the reduced signal propagation speeds within the device at higher temperatures. For example, a 2 GHz microprocessor may be misclassified as a 1.8 GHz device if it overheats during testing. With increasing power dissipation levels, it is becoming more difficult to keep the temperature of the *device under test* (DUT) constant using only passive methods [1–3]. Some form of active control is required for managing the die temperature variation during testing.

Typical functional tests on a microprocessor may last 1–2 min with the power cycling between zero power to full power throughout the test. The form of the test sequence is known in advance, so the power dissipated within the device as a function of time is also known for every device. Most devices under test are packaged devices with interposer and *integrated heat spreader* (IHS) layers, and direct access to the die is not typically available at the testing stage. Therefore, the challenge in the temperature control of a device under test is controlling the die temperature using a control source that can only be applied at another physical point in the system.

Two primary methods have been proposed for the thermal control of an active device during testing. One method [4] utilizes a large thermal mass with embedded heaters and cooling channels in direct contact with the device. The temperature of the thermal mass can be precisely controlled, thereby controlling the temperature of the device under test [5]. This method requires physical contact between the device and the control mass; however, the thermal contact resistance can vary significantly due to the low contact pressures and variations in surface conditions. This variation in contact resistance can make reliable thermal control difficult. The contact resistance variation can be significantly reduced through the use of a thermal interface material (liquid or soft solid), but electronic manufacturers are very resistant to this idea because it requires an additional step to clean the devices after testing,[2] which increases the cost and time of the testing process. In addition, the increased thermal mass of the control system can add significantly to the size of the required heating and cooling systems.

This paper focuses on an alternate approach that uses radiation and convective cooling to control the temperature of the DUT [6]. The convection system is capable of removing the full thermal load produced at 100% device power, but, due to the heat capacitance and flow resistance, the convective cooling cannot be controlled at a rate sufficiently rapid to control the temperature of the device as its power varies during testing. Instead, the convective cooling rate is held constant, and a variable radiation source—a laser—is used to heat the device. By adjusting the radiant heating, the die temperature can be dynamically controlled. This system requires no contact between the device and the control system so the variable thermal contact resistance is no longer a problem. The thermal mass of the system is also kept to a minimum, allowing smaller heating and cooling systems.

We have developed a prototype system that utilizes high performance, air-jet impingement cooling with simultaneous laser heating to control the temperature of a DUT. This system was developed to show the feasibility of a convection/radiation system and to provide initial data for use in the design and layout of a system for use on an actual device test station. A detailed theoretical model of the control scheme has already been given by Sweetland and Lienhard [7] and Richter and Lienhard [8]. The objective of the present experimental study is to control temporal variations in the die temperature. Spatial variations are also an important consideration in improving the test process. While we

[1]The value of the device minimum test temperature and tolerance vary among manufacturers and across device types.

Contributed by the Electrical and Electronic Packaging Division of ASME for publication in the Journal of Electronic Packaging. Manuscript received October 2, 2007; final manuscript received February 10, 2008; published online August 12, 2008. Assoc. Editor: Gamal Refai-Ahmed.

[2]Solid thermal interface materials generally have liquid silicon or some other liquid imbedded in them, which leaves a residue when removed.

 Copyright © 2008 by ASME

Downloaded 18 Aug 2008 to 18.80.0.202. Redistribution subject to ASME license or copyright; see http://www.asme.org/terms/Terms_Use.cfm

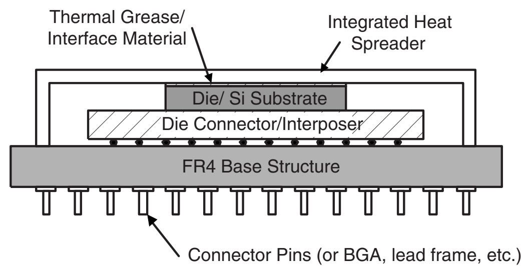

Fig. 1 Typical cross section of a high power microprocessor device. Not all devices will contain all shown components.

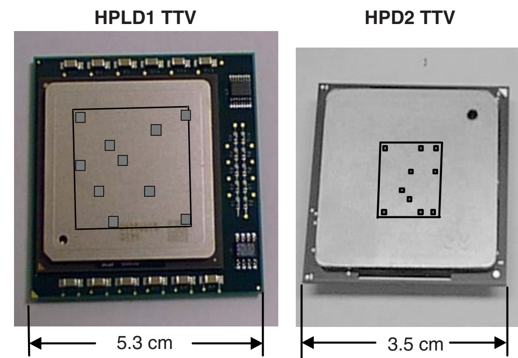

Fig. 2 TTV images with superimposed die and measured RTD positions

provide some information on spatial effects in this study, the control of spatial variation is not the focus of the present work.

2 System Design

The approach taken here was to implement a high performance nozzle cooling system that would be run in a steady state condition. Interspersed within the nozzle array is a fiber optic laser source with sufficient power to enable the real time control of the die temperature for a packaged device. A brief description of a typical DUT follows, with detailed descriptions of the nozzle array, lasers, control system, and test sequences.

2.1 Description of a DUT and Test Sequence. Figure 1 shows a representative device cross section of a typical high power device, which consists of several components. The connections on the base of the device may take several forms, from pins to ball grid arrays to edge mounted lead frames. Not all devices have IHS layers, and there may be multiple interposer layers with no base structure.

In a testing configuration, this device will be held using a suitable fixture and pressed against a test contactor. The test socket is mounted to a *handler interface board* (HIB) that routes each pin to the appropriate testing channel. The back side of the device (HIB side) is not generally accessible for temperature control during testing due to the presence of the interconnects and electronics, so all temperature control methods must be applied to the front face of the device.[3] The handling fixture is custom made for each type of device and must be capable of exerting enough force on the device to ensure reliable contact with the test socket; it is also responsible for the device/socket alignment.

The thermal control system was constructed around two *thermal test vehicles* (TTVs). These devices behave like actual devices, but instead of active components on the silicon die structure, a set of thin film heaters and resistance temperature detector (RTD) temperature sensors on the silicon die mimic thermal loads. Specifically, the HPLD1 thermal test vehicle is a multidie assembly designed for testing high power levels at low to medium power densities. It consists of four thin film heaters on a single monolithic silicon die. For experimental purposes, the four dies were operated in parallel at a single power level for a total die area of 4.2 cm^2. There is a single 1.8 mm thick nickel-coated copper IHS on top of the silicon die with an exposed surface area of 14.9 cm^2, and the base of the die is connected to an interposer structure. The interposer is mounted on an FR-4 base structure that has pin-out connections routed to the thin film heaters and RTD sensors. The other TTV is the HDP2 thermal test vehicle, which is designed for low to medium power levels at high power densities. A single 1.17 cm^2 silicon die with a thin film heater is located beneath a 1.8 mm thick nickel-coated copper heat spreader with a surface area of 9.6 cm^2. There is no interposer structure on the HDP2 TTV, and the die is mounted directly to the FR-4 support structure.

Each device has multiple four-wire RTDs mounted directly on the die structure for the monitoring of the die temperature. Images of the TTVs with a superimposed image of the dies and measured RTD positions are shown in Fig. 2. Both test vehicles are electrically connected to the test system using clam-shell type test sockets, which are mounted to an aluminum base using low thermal conductivity plastic standoffs. This helps produce thermal isolation between the test socket and the mounting base.

A base line test profile of the device power as a function of time is shown in Fig. 3. This base profile can be scaled up or down to obtain any desired peak power magnitude. The profile consists of 0.1 s square waves.

2.2 Convective Cooling System. In order to dissipate the thermal load of a DUT, high rates of convective heat transfer are required. The working fluid is restricted to gases and is further restricted to air or N_2 due to commercial plant equipment and cost considerations. The basic equation for heat transfer from a device is simply $Q=\overline{h}_c A \Delta T$. To increase the total heat transfer Q, we can increase the average convective heat transfer coefficient $\overline{h}_c$ and the available temperature defect ΔT, but not the surface area A, which is fixed for a given device. Increasing the heat transfer by increasing ΔT faces practical limits. If the required ΔT is too large, expensive air chillers may be required. Also as ΔT is increased, since T_{hot} is specified by the device test temperature, T_{cold} might be depressed to the point where condensation and frost formation within the system become a problem. Therefore, the preferred approach is to maximize the convective transfer coefficient $\overline{h}_c$. Two primary methods are commonly used: high velocity cross-flow cooling and impingement cooling.

For the small sizes typical of electronic devices (5×5 cm^2 at the largest), cross-flow cooling[4] can produce $\overline{h}_c$ values on the order of 500 $\text{W/m}^2\,\text{K}$ for Mach numbers, M, less than about 0.5 [9]. At higher flow speeds, noise generation becomes excessive [5]. Also, the need for some type of device retainer can make cross-flow cooling very hard to implement, and cross-flow cooling tends to produce nonuniform cooling across the surface of the device. On the other hand, $\overline{h}_c$ values two to three times greater are possible with impingement cooling.

Martin [10] has compiled an extensive summary of the work done on gas impingement cooling, and we have used his equations to quantify the performance of the nozzle array in the hardware. Based on Martin's correlations, $\overline{h}_c$ values of 1200–1500 $\text{W/m}^2\,\text{K}$ can be easily obtained for $\text{M}<0.5$. Ultimately, the value of $\overline{h}_c$ limits the maximum DUT power for a specific test and air temperature. Since the surface area is fixed, the only way to increase

[3]With component sizes shrinking, devices that may have had open areas on the back side are becoming covered with external interconnects.

[4]Calculation based on fully turbulent flow over the entire width of the device.

Downloaded 18 Aug 2008 to 18.80.0.202. Redistribution subject to ASME license or copyright; see http://www.asme.org/terms/Terms_Use.cfm

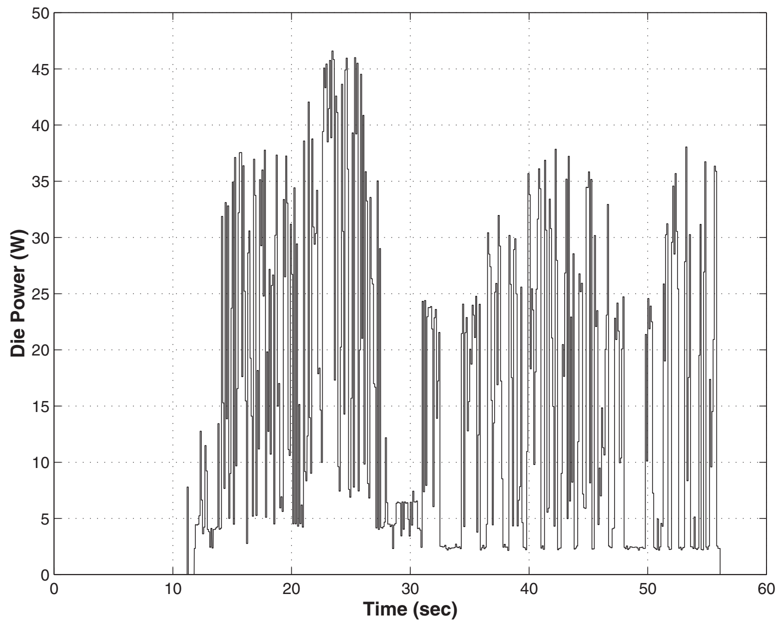

Fig. 3 Base line test power profile. Peak power is 46.6 W. Test sequence consists of 0.1 s square waves.

the maximum DUT power is to increase $\bar{h}_c$ or to decrease the air temperature, which has practical limits as stated earlier. The maximum DUT power has to be calculated based on each DUT and tester configuration. Martin gave the following correlation for an array of round nozzles impinging on a flat plate that yields the following:

$$\frac{\overline{\mathrm{Nu}}}{\mathrm{Pr}^{0.42}} = \left[1 + \left(\frac{H/D}{0.6/\sqrt{f}}\right)^6\right]^{-0.05} \sqrt{f}\frac{1 - 2.2\sqrt{f}}{1 + 0.2(H/D - 6)\sqrt{f}}\mathrm{Re}_D^{2/3} \quad (1)$$

where $\overline{\mathrm{Nu}} = \bar{h}_c D/k_a$ is the average Nusselt number, Pr is the Prandtl number, H is the nozzle to plate spacing, D is the nozzle diameter, and k_a is the conductivity of the air. The Reynolds number Re is

$$\mathrm{Re} = \frac{\rho V D}{\mu} = \frac{\dot{m}}{\mu \pi D} \quad (2)$$

where ρ is the density of the air, V is the velocity, μ is the viscosity of the air, and $\dot{m}$ is the mass flow rate of the air. The geometric factor f is calculated from

$$f = \frac{\pi}{4}\left(\frac{D}{L_t}\right)^2 \quad (3)$$

for an orthogonal array with a nozzle to nozzle spacing of L_t. This correlation is valid under the following conditions:

$$2000 \leq \mathrm{Re}_D \leq 100{,}000 \quad (4)$$

$$0.004 \leq f \leq 0.04 \quad (5)$$

$$2 \leq \frac{H}{D} \leq 12 \quad (6)$$

The nozzle array uses 1.07 mm I.D. polyether-ether-ketone (PEEK) tubing, with an orthogonal array nozzle to nozzle spacing of 7.87 mm and a nozzle to plate distance of 5.9 mm. The nozzle array is constructed from stackable copper modules with two main through holes, one for air and one for water. Seven small holes were drilled through the base of each copper module into the main air channel for mounting the PEEK nozzles. A single nozzle module is shown in Fig. 4 as well as three modules stacked together. These modules can be stacked together to form an array up to seven nozzles wide by any length. When the modules are clamped

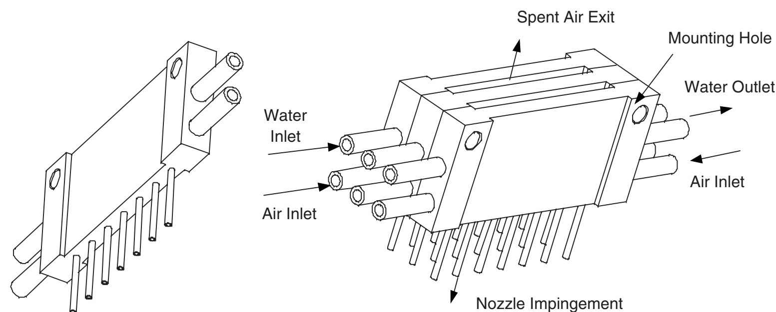

Fig. 4 Single and stacked nozzle modules. Number of nozzles in the array could be varied by changing the number of modules and by blocking off specific nozzle mounting holes.

Downloaded 18 Aug 2008 to 18.80.0.202. Redistribution subject to ASME license or copyright; see http://www.asme.org/terms/Terms_Use.cfm

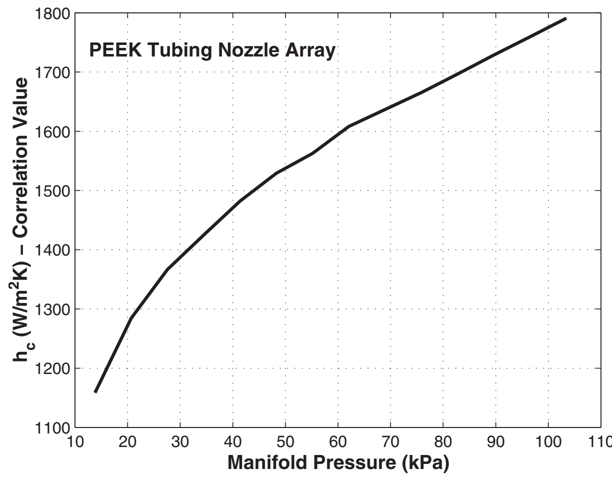

Fig. 5 Manifold pressure versus $\bar{h}_c$ for the prototype system. A 5×5 nozzle array was used with the HPLD1 TTV and a 3×3 nozzle array was used with the HPD2 TTV.

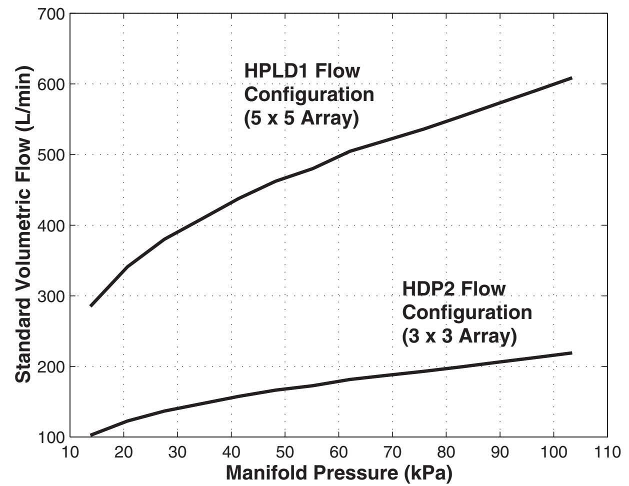

Fig. 6 Volumetric flow rate versus the manifold pressure under standard conditions (101.36 kPa and 21.4°C) for the 5×5 nozzle array used with the HPLD1 TTV and the 3×3 nozzle array used with the HPD2 TTV

together, a 3.05 mm slot is formed between them, since the ends of each module are wider than the center section. These slots provide spent air exits for the nozzle air and act as an access point for fiber optics and radiation sources. The copper tubing was silver soldered onto the air and water channels on each end of each module. The end of each copper tube was fitted with a compression fitting to allow a connection to the distributed air and water systems.

The actual number of nozzles used depended on which specific test device was mounted in the test socket. For the HPLD1 TTV, the nozzle array was reduced to a 5×5 array of nozzles, centered over the IHS. For the HDP2 TTV, the nozzle array was further reduced to a 3×3 array, centered over the IHS. While impingement cooling could have been extended to the edges of the interposer/base structure and test socket, these smaller limited arrays were capable of removing any thermal load generated by the particular TTVs tested. Compressed laboratory air was supplied to keep the manifold pressure constant within ±344 Pa for any specific manifold pressure between 13.8 kPa and 206.8 kPa. While connections for the secondary water cooling of the copper nozzle stacks were included (for very high device powers and low $\bar{h}_c$), these connections were never used.

Figure 5 shows $\bar{h}_c$ as a function of manifold pressure for the prototype system, as calculated from Martin's equations. This plot is valid for both the HPLD1 TTV and the HDP2 TTV as the nozzle configuration is the same.[5] Figure 6 shows the volumetric flow rate under standard conditions versus the manifold pressure for the nozzle arrays for the HPLD1 and HDP2 thermal test vehicles.

2.3 Lasers and Optics. There are only a few wavelengths at which high power thermal radiation sources can be purchased as standard components. These sources are CO_2 lasers, Nd:YAG (yttrium aluminum garnet) lasers, high output diode laser bars, and noncoherent sources (tungsten lamps, quartz-tungsten-halogen (QTH) bulbs, and arc-lamps). The last choice, noncoherent sources, is not really practical for application to the thermal control of a DUT because their output is diffused and must be concentrated on the target using reflector assemblies too large for the test configuration [11]. IR bulbs also have slow response times[6] making them impractical for high speed control. Arc-lamps have very fast response times, but tend to have high levels of RF noise, which will interfere with the electrical testing. The only viable choice for this application at present are lasers.

The specific laser chosen will depend on the specific device to be tested. Table 1 summarizes the basic reflectivity and absorption coefficients of devices at commonly available wavelengths. The desired values for the best performance are a very low reflectivity and an absorption coefficient that will distribute the energy absorbed only within the encapsulating layer. In all situations, the propagation of the radiation through the encapsulant or substrate to the active components on the die must be avoided, so as to prevent permanent damage to the device or the generation of photocurrents (such photocurrents would interfere with the device operation and cause failure during the testing cycle).

Metals have very high absorption coefficients but generally also have very high reflection losses, making the laser heating of large areas more difficult. Actual ρ values are strongly dependent on surface conditions and can vary by 40–50% for a given material.

[5]The number of nozzles for each TTV is different, but the spacing, nozzle diameter, and offsets are identical, so for the same Reynolds number (or manifold pressure) the convection coefficient is the same.

[6]A fast IR bulb typically has a 1–3 s settling time to reach 90% of the steady state.

Table 1 Reflectivity and absorption coefficients for common device materials

Material Type	Diode laser 790–980 nm	Nd:YAG laser 1.06 μm	CO_2 laser 10.6 μm
Silicon [16]	$\rho\approx 0.3$ $\kappa\approx 10^4$ cm^{-1}	$\rho\approx 0.3$ $\kappa\approx 1.5$ cm^{-1}	$\rho\approx 0.2-0.7$ [a] $\kappa\approx 1.5$ cm^{-1}
Al_2O_3 [b] [16]	$\rho\approx 0.8-0.9$ $\kappa\approx 0.009$ cm^{-1}	$\rho\approx 0.9-1.0$ $\kappa\approx 0.009$ cm^{-1}	$\rho\approx 0.1-0.15$ $\kappa\geq 100$ cm^{-1}
SiO_2 [c] [16]	$\rho\approx 0.8-0.9$ $\kappa\approx 0.004$ cm^{-1}	$\rho\approx 0.9-0.95$ $\kappa\approx 0.004$ cm^{-1}	$\rho\approx 0.1-0.2$ $\kappa\geq 100$ cm^{-1}
Polyimide Plastics[d] [17]	$\rho\approx 0.2$ $\kappa\approx 10-20$ cm^{-1}	$\rho\approx 0.2$ $\kappa\approx 10-20$ cm^{-1}	$\rho\approx 0.1$ $\kappa\approx 300-700$ cm^{-1}
Ni coated Cu[e] [18]	$\rho\approx 0.6$ $\kappa\approx 10^5$ cm^{-1}	$\rho\approx 0.8$ $\kappa\approx 10^5$ cm^{-1}	$\rho\approx 0.95$ $\kappa\approx 10^5$ cm^{-1}

[a]Highly dependent on doping type and quantity.
[b]Crystalline.
[c]Fused.
[d]Representative values only. Actual values strong function of specific plastic composition.
[e]ρ values are a strong function of surface conditions

Downloaded 18 Aug 2008 to 18.80.0.202. Redistribution subject to ASME license or copyright; see http://www.asme.org/terms/Terms_Use.cfm

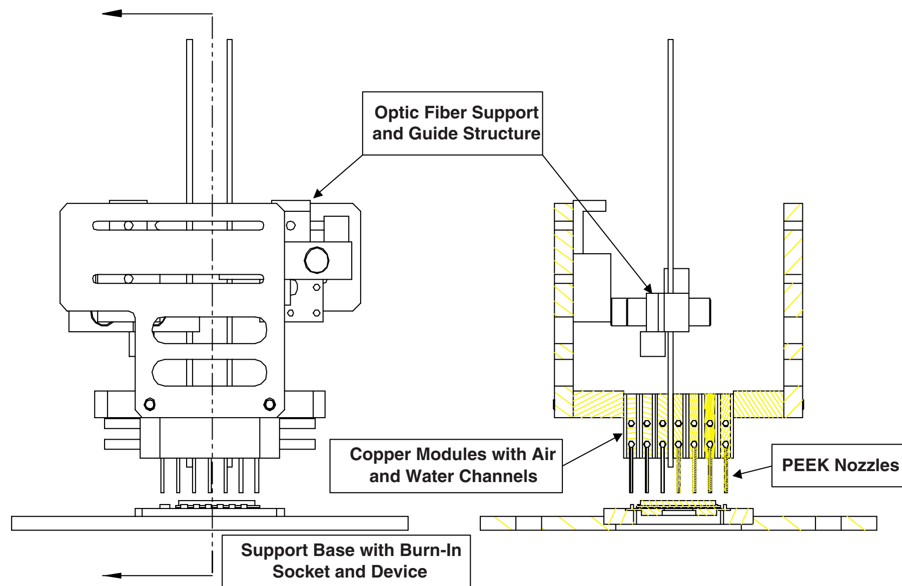

Fig. 7 Side view and cross sectional view of assembled laser/convection system. Manifold system and base support structures are not shown.

The energy that is not reflected is absorbed over a very small region below the surface. Exposed silicon devices are semitransparent to wavelengths above 1 μm but have a very high absorption coefficient below 1 μm. This makes a diode laser the obvious choice for heating exposed silicon devices. High system efficiency is desired to reduce the thermal load imposed on the overall control system by the radiation source. CO_2 and Nd:YAG lasers are both around 20% efficient, while diode lasers can be up to 35–40% efficient.

The lasers selected for our system were a pair of 60 W fiber optic coupled diode lasers operating at 811 nm. The power level could be controlled from zero to 100% power through an externally applied analog voltage. Each laser consists of two 30 W diode bars connected to fiber optic bundles. The fiber bundle from each diode is routed to a fiber optic splice and from there into an optical connector with an SMA-905 type output connection for linking to a fiber optic pigtail. Typical losses in the SMA type connector are about 1.0 dB. The fiber optic pigtails used are 1000 μm diameter pure silica core fibers, 3.5 m in length with a 1400 μm coated diameter. Power pigtails were used for the final power delivery to allow for flexibility in laser placement, and more importantly, as a means of protecting the fiber optics in the laser units. If a fiber pigtail is damaged in handling or operation, it can be removed and replaced. Also, the use of fiber pigtails enables the quick replacement of a laser source in case of a diode failure. Laser diodes typically have run times in the thousands of hours, which are sufficient for testing 50,000 or more DUTs, depending on the test sequence, before maintenance requirements dictate a system changeover.

The fiber pigtails used were of two standard types. One type had a cleaved tip end and the other had a full radius tip. The cleaved tip fiber produced an output beam divergence of 12 deg included angle. The radius tip fiber produced a 170–180 deg beam divergence, which made it difficult to limit the illumination spot to the surface of the device, resulting in high losses. Custom ground fiber tips were also available, but were not used owing to their high cost.

A key design objective was to minimize the number of optical components and interfaces in order to minimize the power loss between the diode lasers and the device. The system also had to be designed with consideration to the manufacturing environment. The test heads in which this system would typically be mounted are subject to vibrations and possibly high shock loads as devices are loaded and unloaded from the test socket. Keeping a precise optical focus would consequently pose major problems for long term reliability. These design requirements result in low cost fiber optic pigtails being the best choice for illuminating the surface of the DUT.

The optical fibers from the lasers can be run through any of the slots of the nozzle modules, either vertically or at an angle. This allows a great deal of flexibility in positioning the fiber optics over the test socket. Moving each fiber closer to the device surface reduces the size of the illumination spot. The maximum spot size is limited by how far the end of the fiber can be positioned from the surface. If the fiber is pulled back too far, the laser beam may intersect the end of the cooling nozzles, which would cause damage; alternatively, with very short nozzle lengths, the beam may be shielded by the sides of the nozzle modules. The design becomes a trade-off between small nozzle spacing in order to obtain maximum convective cooling performance and a large laser illumination spot size. A schematic diagram of the assembled system is shown in Fig. 7.

2.4 Data Acquisition System. An Agilent HP34970A data acquisition/DMM system was used with the 20-channel Agilent HP34901A multiplexer units for temperature measurements and one control module. The data channels monitored consist of temperature measurements from the RTDs mounted on the die structure of each thermal test vehicle. The HPLD1 die has 13 four wire RTDs, ten of which are routed to external pins and the DAQ system, while the HDP2 TTV has all ten RTDs routed to external pin connections and the DAQ system. Each multiplexer module has a built in cold-junction reference accurate to 0.8°C [12] and repeatable to 0.1°C. To reduce measurement error, all thermocouples were connected to the same multiplexer module. For the sampling rate, the DAQ system could be run in one of two modes. If data were acquired on all temperature channels, the system would complete a full channel scan in 0.67 s. If the data were acquired on a single channel at a time, then the effective sampling rate was 40 Hz.

2.5 Power Supply and Control System. The thermal test vehicles were powered by an Agilent 6627A four-channel dc power supply. Each channel is capable of producing 40 W at a peak voltage of 50 V at 0.8 A [13]. The actual wiring depended on which TTV was being run and under which configuration. The

Downloaded 18 Aug 2008 to 18.80.0.202. Redistribution subject to ASME license or copyright; see http://www.asme.org/terms/Terms_Use.cfm

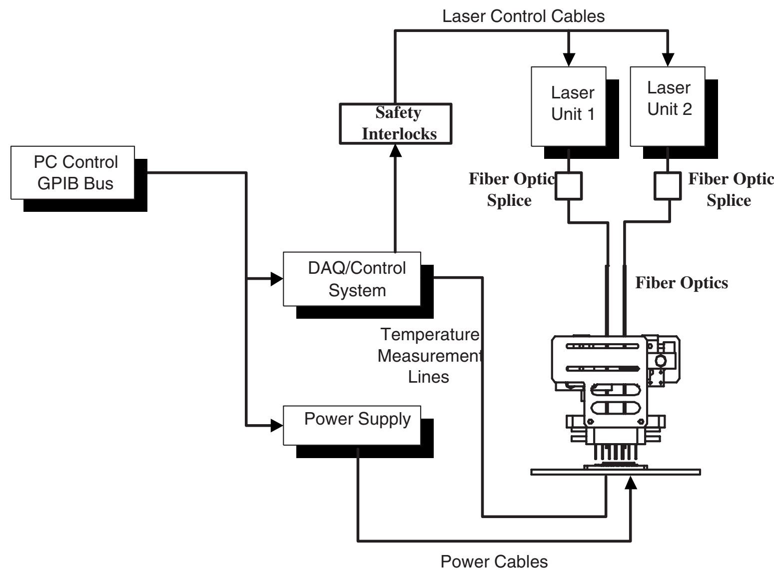

Fig. 8 Schematic diagram of the control and data acquisition systems for laser/convection prototype system

HDP2 TTV had a single configuration where two of the dc output channels were slaved together. This provided up to 80 W at 1.6 A of current at a common voltage to the single die heater. The voltage was set in the power supply control input, and remote sensing lines were used to correct for supply and return line resistance between the power supply and pin connections on the test socket. For the HPLD1 TTV, dc supply Channels 1 and 2 were slaved together and Channels 3 and 4 were slaved together. One of these outputs was connected to die Heaters 2 and 3 in parallel, while the other output channel was connected to die Heaters 1 and 4 in parallel. This configuration allowed for uniform high power dissipation in the die at total power levels of up to 140 W.

System control was provided by a personal computer (PC) system connected through a general purpose interface bus (GPIB) interfaced to the power supply and DAQ system. A schematic diagram of the control and the DAQ system is shown in Fig. 8. The power supply was limited to a 10 Hz update rate, while the DAQ sampling frequency was based on the number of channels for a particular configuration.

3 TTV Calibration and Test Procedures

Both the RTD sensors and the thin film heaters on the thermal test vehicles were calibrated by measuring the resistance at two reference temperatures. The two reference temperatures used for calibration were the room temperature and a hot temperature close to the expected maximum operating temperature of the system. In order to reduce the error in the calibration measurement, an insulated chamber was constructed in which the entire base, socket, and device could be placed. The system was allowed to reach equilibrium overnight in a sealed room with all sources of air movement turned off. The next morning, resistance readings from each RTD were taken at a rate of 1/s over 15 min. These resistance values for each channel were averaged and used for the room temperature data point. Four T-type thermocouples were also mounted in the chamber to provide the reference room temperature.

The high temperature reference point was obtained by connecting the sealed chamber to an air forcing unit. The unit was capable of providing air at a constant high temperature within $\pm 0.5^\circ\mathrm{C}$ of a specified set point. A small vent hole was opened on the top of the chamber to permit air circulation, and the whole system was turned on and allowed to run for 6–8 h to reach equilibrium. At this point, resistance and temperature measurements were taken over a 15 min period and averaged values were used as the high temperature calibration point.[7] The two data points were then used to generate a scaling and offset value for each RTD on each TTV assembly. The data for each TTV were used to generate a calibration file that was loaded each time the TTV in the test socket was changed.

In the same manner and at the same time as RTD resistances, the resistance of each thin film heater was measured using a four wire sensor at two reference temperature points to obtain a calibration for the variation of die resistance with temperature. This information was used to generate a voltage driving file for a specified die temperature and die power profile. Real time measurement of the device power was not possible due to the high currents and limited DAQ channel availability. Only two devices of each TTV type (HPLD1 and HPD2) were available for testing purposes, and this calibration was performed on each device. With the calibration files for the die power and the RTD calibration for each device, each device of each TTV type behaved the same as the other device once installed in the test socket.

The accuracy of temperature measurement on the TTV die structures was a function of a number of factors. Since the measurement of interest was the relative temperature change, absolute errors in temperature were neglected. The rms error in temperature change was a function of the resolution and accuracy of resistance measurement and of the accuracy of calibration files. Using standard propagation of uncertainty [14], the repeatability in the measured temperature change was found to be $0.01^\circ\mathrm{C}$, which agrees with the typically cited measurement performance of commercially available RTD assemblies.

3.1 TTV Power Accuracy. The error in the power profile can be calculated in a manner similar to the temperature measurement error, but there was the additional complication that the error was dependent on the performance of the temperature control (i.e., test runs where temperature control was not used or was not effective). In a similar manner to the RTD resistance, the calibration values were obtained for the resistances of the thin film heaters. The goal was to determine the film resistance as a function of temperature and to use this information along with the known voltage driving

[7]The actual high temperature point varied over the range of devices due to external losses. The range varied from $70^\circ\mathrm{C}$ to $75^\circ\mathrm{C}$ with an air forcing temperature of $85^\circ\mathrm{C}$.

Downloaded 18 Aug 2008 to 18.80.0.202. Redistribution subject to ASME license or copyright; see http://www.asme.org/terms/Terms_Use.cfm

file[8] to determine the error in the actual device power.

The error in the die temperature was the largest source of error in the calculation of the device power because of the effect on the die resistance. The actual operating temperature was generally unknown until after several runs were made and then only to within 2°C. The error in die power became significant in those cases in which no form of temperature control was used, so that the die temperature would vary by 20–30°C over the run. For temperature controlled test sequences, where the die temperature could be controlled to within ±2°C, the instantaneous error in die power was no more than ±6%. For uncontrolled tests with a die temperature variation of ±10°C, the instantaneous error could reach ±26%. Based on the equipment available for this testing, it was not possible to set up a feedback loop that automatically compensated for the error in die power without reducing the system update rate to below a 1 Hz level. This rate would have been too slow to obtain any meaningful test data.

3.2 Test Procedure. The entire system was run from a single PC via a graphical user interface in which all parameters were set before a test began. In a factory test environment, the DUT would be preheated to the required test temperature before being inserted into the test socket. Upon initiation of the test, the cooling system would be initialized at the same time as the electrical test in order to keep the temperature of the device uniform. Because the convective cooling of the prototype system was not controlled by the computer and no method of preheating the device to the correct test temperature was available, the test sequence was modified slightly. In order to bring the TTV's temperature up before a test, the nozzle cooling system would be turned on. The power supply for each film heater would then be powered up at the peak power of the test sequence and the device would be allowed to reach a steady temperature. Once this steady state was obtained, the power profiles for the die and lasers would be started along with the data acquisition system for temperature measurement. At the end of the test sequence, the lasers would be turned off and the peak die power would again be turned on at the peak test value to maintain the die temperature at the target value. This was the best method for simulating actual test conditions where the devices are preheated, and the test sockets are maintained at the target temperature [2,15]. The same results could have been obtained by leaving the film heaters without power and preheating the DUT using the laser systems. Preheating through the film heaters was chosen to minimize the operating time of the laser diodes.

4 Experimental Results

The HDP2 TTV was designed for low to medium power levels at much higher densities than the HPLD1 TTV device. The peak electrical power running through the die was 56 W. Figure 9 shows the die temperature response of a HDP2 TTV to a 23.3 W peak power test sequence with the nozzle manifold pressure set at 41.37 kPa and with no active temperature control. As can be seen, the temperature variation of the die over the test sequence is over 20°C. In order to meet testing specifications, the die would have to be preheated to a chosen minimum test temperature (85°C) and the temperature variation during the test with no active control could potentially drive the die temperature up to 105°C. Figure 9 shows the die temperature response as measured by all ten RTD temperature sensors. The spatial variation across the die during an uncontrolled test sequence can be seen. The variation across the different sensors before the test sequence begins is less than 0.04°C and during the active test sequence, the spatial variation at any given instant of time is less than 4°C.

The base test sequence can be scaled up and down to see the effect of changing the peak die power levels. Figure 10 shows the temperature response of a HDP2 TTV with a fixed manifold pressure of 41.37 kPa, as the peak power is changed. The data presented are from a single RTD sensor and represent the sensor closest to the center mass of the die. The die power fluctuations started at time $t=20$ s and finished at time $t=67$ s. The die power was turned off before and after these times. The convective cooling jets were turned on well before test initiation and left on until well after test completion. The uniform temperature before the die power was turned on and the approach to uniformity after the completion of the test run are due to this constant forced convection state with no die power applied to the system. As can be seen in Fig. 10, the general shape of the temperature variation remains the same with varying manifold pressures, but the magnitude of the die temperature change increases with increasing die peak power. The effect of changing the manifold pressure with a constant power sequence is shown in Fig. 11. For a fixed die peak power, changing the value of $\bar{h}_c$ over the range of 1250–1700 $\mathrm{W/m^2\,K}$ by changing the manifold supply pressure has relatively little effect on the total die temperature variation.

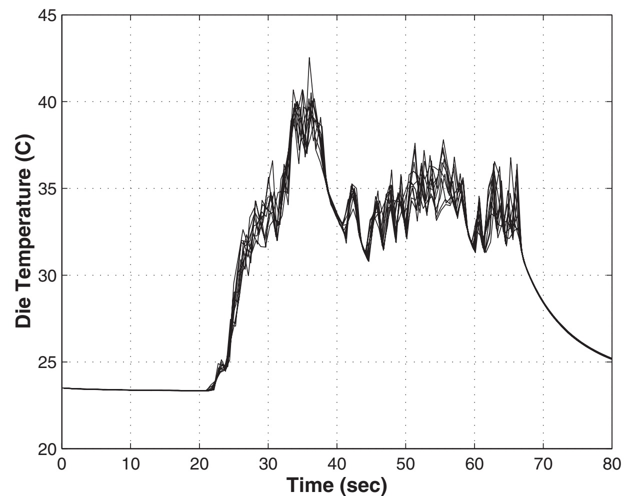

Fig. 9 Uncontrolled die temperature for a HDP2 TTV subject to a 23.3 W peak die power test sequence with a 41.37 kPa manifold pressure for the nozzle cooling system. The die temperature data are from all ten RTD sensors.

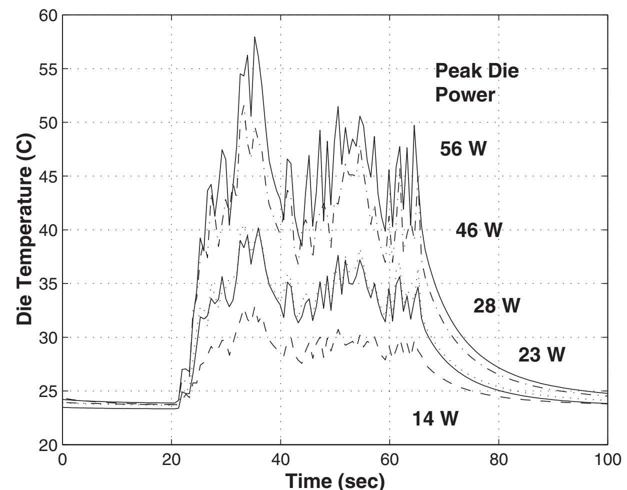

Fig. 10 Uncontrolled die temperature for a HDP2 TTV subject to various peak die power scaled test sequences with a constant manifold supply pressure of 41.37 kPa. Data are from a single die centered RTD channel for peak die powers of 14 W, 23 W, 28 W, 46 W, and 56 W.

[8]Supply voltage was known to an accuracy of ±50 mV [13].

Downloaded 18 Aug 2008 to 18.80.0.202. Redistribution subject to ASME license or copyright; see http://www.asme.org/terms/Terms_Use.cfm

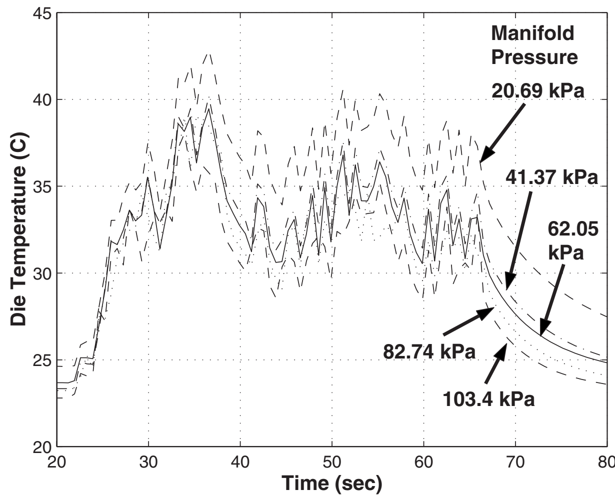

Fig. 11 Uncontrolled die temperature for a HDP2 TTV subject to the same 23.3 W peak die power test sequence with nozzle cooling system manifold pressures of 20.69 kPa, 41.37 kPa, 62.05 kPa, 82.74 kPa, and 103.4 kPa. Data are from a single die centered RTD channel for each pressure.

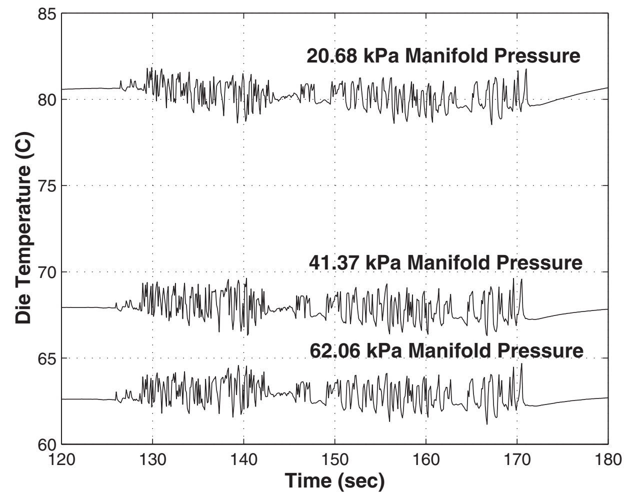

Fig. 13 Controlled die temperatures for a PDP2 TTV subject to a 23.3 W peak die power test sequence at cooling nozzle manifold pressures of 20.68 kPa, 41.37 kPa, and 62.06 kPa. Data represent a single die centered RTD channel.

This demonstrates that just increasing the cooling capability does not significantly improve the die temperature response.

Figure 12 plots the temperature response with and without active temperature control for a HDP2 TTV subjected to a 46.7 W peak power test sequence. This plot clearly shows the effectiveness of the laser/convection temperature control system. The minimum temperature of each sequence would be adjusted to the target temperature (e.g., 85°C, for example) by changing either the manifold air temperature or the manifold supply pressure. The objective of the control system was to minimize the die temperature variation above this specified minimum temperature. In the uncontrolled case, this represents a temperature change of about 29°C, while the control variation is less than 4°C. The effect of changing the manifold pressure on the controlled temperature response of the DUT is shown in Fig. 13. All three plots are for a HPD2 TTV with a 23.3 W peak die power test profile but with three different manifold pressures. Changing the supply pressure changed the mean temperature but had almost no effect on the magnitude of the controlled temperature variation of the die during the test. This clearly demonstrates that the convection cooling affects the mean temperature of the die during the test, but the radiation control affects the temperature variation of the die during the test sequence.

Figure 14 plots the controlled die temperature response of a HDP2 TTV subjected to a 46.7 W peak power test sequence with the manifold pressure set at 41.37 kPa. The data are for all ten temperature sensors during a single run in order to see the spatial temperature variations of the die using active temperature control. Unlike the die temperature response in the uncontrolled case shown in Fig. 9, the initial temperature profile of the die is not uniform. The initial spatial variation across the die is 2°C. This is due to the nonuniform illumination of the IHS surface using the two diode laser sources. The maximum spatial variation at any given instant of time during the active test is less than 4.5°C, but the total peak to peak variation across all sensors for the duration of the active test sequence is 5.5°C. This is still far less than the 20°C temperature variation of the die when no active control is used.

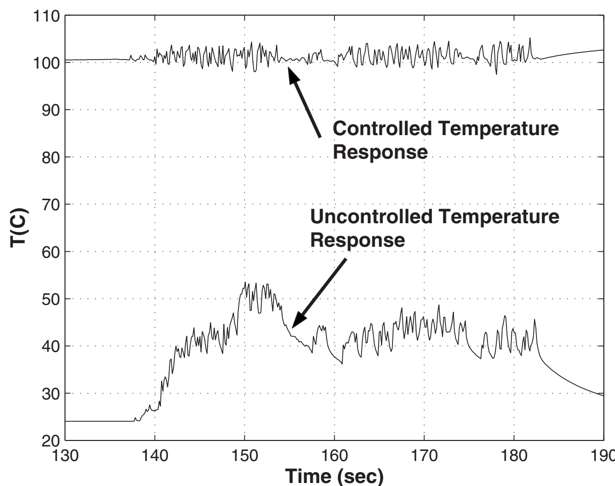

Fig. 12 Uncontrolled and controlled die temperatures for a HDP2 TTV subject to a 46.7 W peak die power test sequence with a 41.37 kPa nozzle cooling system manifold pressure. Data represent a single die centered RTD channel.

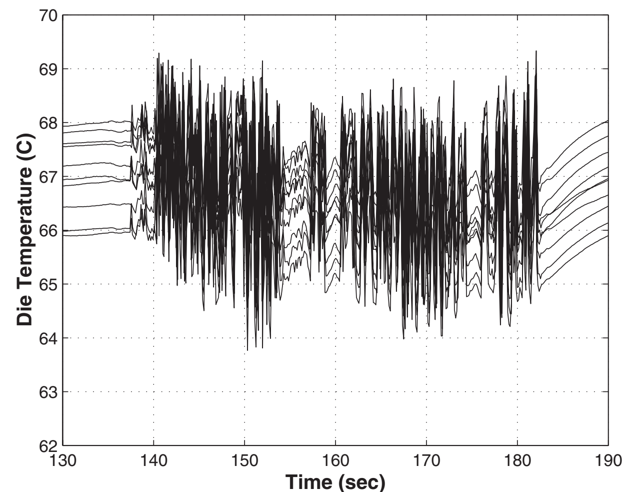

Fig. 14 Controlled die temperature for HDP2 TTV subject to a 23.3 W peak die power test sequence with a 41.37 kPa manifold pressure for the nozzle cooling system. The die temperature data are from all ten RTD sensors.

Downloaded 18 Aug 2008 to 18.80.0.202. Redistribution subject to ASME license or copyright; see http://www.asme.org/terms/Terms_Use.cfm

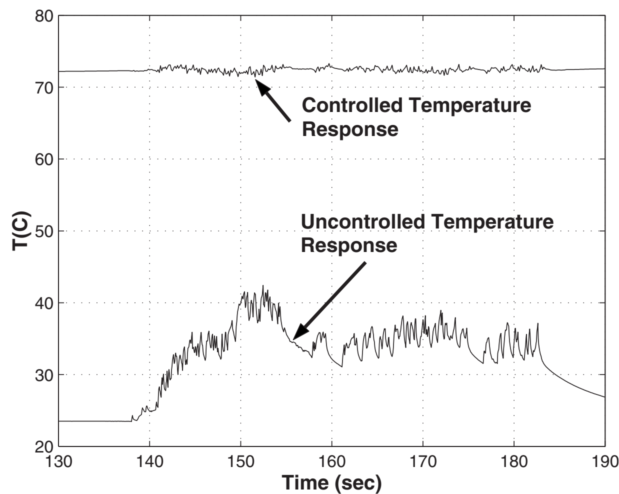

Fig. 15 Uncontrolled and controlled die temperatures for a HPLD1 TTV to a 46.7 W peak die power test sequence with 41.37 kPa cooling nozzle manifold pressure. Data represent a single die centered RTD channel.

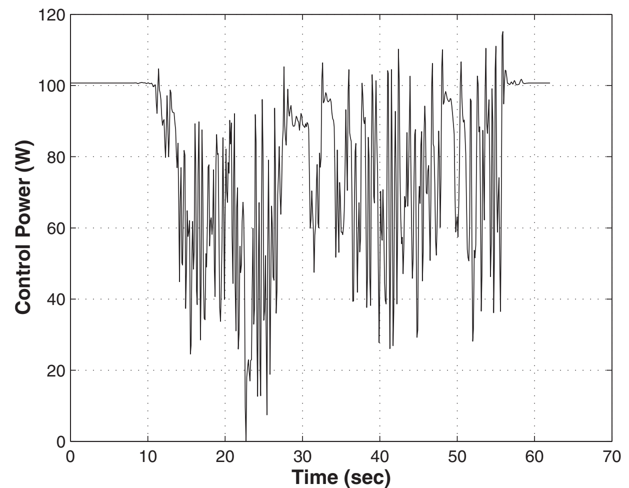

Fig. 17 Control power sequence for HPLD1 TTV controlled temperature response shown in Fig. 15

The HPLD1 TTV was designed for medium to high power levels at lower densities than the HDP2 TTV device. Figure 15 plots the temperature response with and without active temperature control for HPLD1 TTV subjected to a 46.7 W test sequence. Again, this plot shows the effectiveness of the laser/convection temperature control system. A detailed view of the controlled temperature response in Fig. 15 can be seen in Fig. 16. The uncontrolled temperature change of the die is 20°C, while the controlled temperature response of the die is 1.6°C. The control sequence used to obtain this response is shown in Fig. 17. The spatial temperature variation at a given instant in time of the HPLD1 TTV during a 46.7 W test sequence with a 41.37 kPa manifold pressure was just over 4°C in the uncontrolled sequence and was 6.5°C during the controlled test sequence. This higher spatial variation in the controlled state of the HPLD1 TTV compared to the HPD2 TTV was due to the larger die size and the increased difficulty in generating a uniform surface illumination using the two laser sources. Even with the spatial variation of the die in the controlled state, the overall die temperature variation in the controlled state is significantly less than a single point temporal variation in the uncontrolled state.

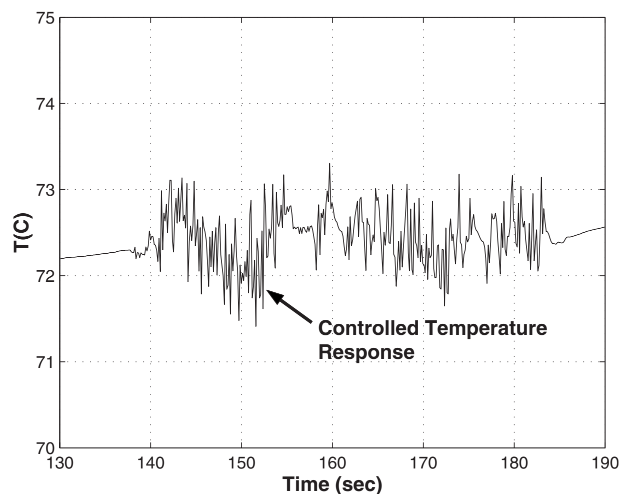

Fig. 16 Detailed view of controlled die temperature for a HPLD1 TTV to a 46.7 W peak die power test sequence with 41.37 kPa cooling nozzle manifold pressure. Data represent a single die centered RTD channel.

Unfortunately there are no available data for comparison with other control techniques (active or passive) for these TTVs; however, these results clearly demonstrate that radiation/convection systems can be used for the active control of DUT temperatures during the testing process. The results from this feasibility study can be used in the design of an actual test head for use on active device testers. This will provide data that can be compared with results from passive temperature control systems as well as other active systems that are currently being designed.

5 Future Work

We have demonstrated the effectiveness of active temperature control of DUT using a combined convection/radiation control scheme. While the basic validity of this type of approach has been proven, significantly more work and data are required for the full commercial development of this type of system. This work includes the testing of actual production parts in order to understand the effects of device to device variation on the final die temperature. Variations in die and component sizes, actual operating powers, long term stability of cooling performance, and variations in laser output will all affect the final die temperature tolerance that can be maintained. The effect of spatial variations also requires significant study. Using multiple independent radiation sources has the potential to better control the spatial temperature variations of the DUT as well as the time based variations. The study of these effects is beyond the scope of this current work. Also, initial models and experimental data were based on the assumption of uniform die temperatures across the width on each die. Temperature uniformity across the die is affected by the uniformity of the cooling, the die position relative to the IHS, the location of the laser heating on the surface, as well as the internal heat generation within the device itself. Both TTV types were set up with uniform generation across the thin film resistive die structures. The variation in the die temperatures in the experimental data is due to the three dimensional conduction effects in the IHS as well as the laser illumination spot size and location. The lasers were set up for complete and uniform coverage over the die area only, not over the entire surface of the IHS so lateral conduction effects also affected the die temperature uniformity. In actual devices, the generation of heat within the die is often nonuniform. This will also affect the die temperature spatial and time uniformity.

Downloaded 18 Aug 2008 to 18.80.0.202. Redistribution subject to ASME license or copyright; see http://www.asme.org/terms/Terms_Use.cfm

6 Summary and Conclusions

A new concept for active thermal control of high-powered devices under testing has been implemented. The system uses high performance, air-jet impingement cooling with simultaneous laser heating to dynamically control the temperature of devices under typical test conditions.[9] The experimental results clearly demonstrate that a convection/radiation control system is capable of reducing the time variations in die temperature during a typical test sequence. Depending on the configuration of the DUT, the test sequence, the cooling system, and the laser system, the variation in die temperature can be reduced up to an order of magnitude at select locations. This paper presented results for a packaged die with integrated copper heat spreaders. For other device configurations, the design of the control system must be modified following the approach described. The cooling and laser power requirements will depend largely on the test sequence design. The range of device power densities that can be controlled using this type of system is limited only by the available radiation power and by the cooling performance of the nozzle system.

Acknowledgment

The authors would like to thank Teradyne Inc. for financial support of this work and Intel Corporation for providing test samples. The authors would also like to thank Andreas Pfahnl and Ray Mirkhani of Teradyne for their technical support of this work, as well as Pooya Tadayon at Intel for information and advice on testing conditions.

Nomenclature

Symbol Description

A = convection surface area (m^2)
D = nozzle diameter (m)
f = nozzle geometry form factor
$\bar{h}_c$ = average convective transfer coefficient (W/m^2 K)
H = nozzle to plate spacing (m)
k_a = thermal conductivity of air (W/m K)
L_t = nozzle to nozzle spacing for orthogonal array (m)
M = Mach number
$\dot{m}$ = mass flow rate of air (kg/s)
$\overline{\mathrm{Nu}}$ = average Nusselt number
Pr = Prandtl number
Q = convective heat transfer (W)
Re_D = Reynolds number
ΔT = convection temperature defect (K)
V = velocity of air (m/s)

Greek Symbols

κ = absorption coefficient (cm^{-1})
μ = viscosity of air (kg/m s)
ρ = surface reflectivity
ρ = density of air (kg/m^3)

[9]Teradyne, Inc. has a patent pending on this system.

References

[1] Pfahnl, A. C., Lienhard V, J. H., and Slocum, A. H., 1998, "Temperature Control of a Handler Test Interface," *Proceedings of the IEEE International Test Conference*, IEEE Computer Society, Washington, DC.
[2] Pfahnl, A. C., Lienhard V, J. H., and Slocum, A. H., 1999, "Thermal Management and Control in Testing Packaged Integrated Circuit Devices," *Proceedings of the 34th Intersociety Energy Conversion Conference*, Vancouver, BC, Am. Nuclear Society, LaGrange Park, IL.
[3] Malinoski, M., Maveety, J., Knostman, S., and Jones, T., 1998, "A Test Site Thermal Control System for at-Speed Manufacturing Testing," *Proceedings of the IEEE International Test Conference*, IEEE Computer Society, Washington, DC, , pp. 119–128.
[4] Tustantswkyj, J., and Babcock, J. B., 1998, "Temperature Control System for an Electronic Device Which Achieves a Quick Response by Interposing a Heater Between the Device and a Heat Sink," U.S. Patent No. 5,821,505.
[5] Tustaniwskyj, J. I., and Babcock, J. W., 1997, "Constant Temperature Control of a Device Under Test (DUT)—Part I," Adv. Electron. Packag., **2**, pp. 2031–2036.
[6] Sweetland, M., 2001, "Design of Thermal Control Systems for Testing of Electronics," Ph.D. thesis, Massachusetts Institute of Technology, Cambridge.
[7] Sweetland, M., and Lienhard V, J. H., 2003, "Active Thermal Control of Distributed Parameter Systems With Application to Testing of Packaged IC Devices," ASME J. Heat Transfer, **125**(1), pp. 164–174.
[8] Richter, C. C., and Lienhard, J. H., V, 2006, "Active Thermal Control of Distributed Parameter Systems Excited at Multiple Frequencies," ASME J. Heat Transfer, **128**(1), pp. 93–99.
[9] Mills, A. F., 1995, *Heat and Mass Transfer*, Irwin, Chicago.
[10] Martin, H., 1977, "Heat and Mass Transfer Between Impinging Gas Jets and Solid Surfaces," *Advances in Heat Transfer*, T. Irvine and J. P. Hartnett, eds., Academic, New York, Vol. 13, pp. 1–60.
[11] Sweetland, M., and Lienhard V, J. H., 2001, "Rapid IR Heating of Electronic Components in the Test Cycle," *Proceedings of the 35th National Heat Transfer Conference*, Anaheim, CA, ASME, New York.
[12] 1999, Agilent 34970A Data Acquisition/Switch Unit—User's Guide.
[13] 2000, Agilent 6627A Multiple Output Linear System DC Power Supply—User's Guide.
[14] Taylor, J. R., 1982, *An Introduction to Error Analysis*, University Science Books, Mill Valley, CA.
[15] Pfahnl, A. C., Lienhard V, J. H., and Slocum, A. H., 1998, "Heat Transfer Enhancing Features for Test Handler Trays," IEEE Trans. Compon., Packag., Manuf. Technol., Part C, **21**(4), pp. 302–310.
[16] Touloukian, Y. S., and Dewitt, D. P., 1970, "Thermal Radiative Properties: Non-Metallic Solids," *Thermophysical Properties of Matter*, Plenum, New York, Vol. 8.
[17] Wang, Y., Abe, Y., Matsuura, Y., Miyagi M., and Uyama, H., 1998, "Refractive Indicies and Extinction Coefficients of Polymers for the Mid-Infrared Region," Appl. Opt., **37**(30), pp. 7091–7095.
[18] Ordal, M. A., Long, L. L., Bell, R. J., Bell, S. E., Bell, R. R., Alexander, R. W., and Ward, C. A., 1983, "Optical Properties of the Metals Al, Co, Cu, Au, Fe, Pb, Ni, Pd, Pt Ag, Ti, and W in the Infrared and Far Infrared," Appl. Opt., **22**(7), pp. 1099–1119.

Downloaded 18 Aug 2008 to 18.80.0.202. Redistribution subject to ASME license or copyright; see http://www.asme.org/terms/Terms_Use.cfm